

A monohydride high-index silicon surface: Si(114):H-(2×1)

A. Laracuente,^{a)} S. C. Erwin, and L. J. Whitman

Naval Research Laboratory, Washington, DC 20375-5342

(Received 17 November 1998; accepted for publication 12 January 1999)

We describe the adsorption of H on Si(114)-(2×1) as characterized by scanning tunneling microscopy and first-principles calculations. Like Si(001)—and despite the relative complexity of the (114) structure—a well-ordered, low-defect-density monohydride surface forms at ~400 °C. Surprisingly, the clean surface reconstruction is essentially maintained on the (2×1) monohydride surface, composed of dimers, rebonded double-layer steps, and nonrebonded double-layer steps, with each surface atom terminated by a single H. This H-passivated surface can also be easily and uniformly patterned by selectively desorbing the H with low-voltage electrons. © 1999 American Institute of Physics. [S0003-6951(99)04010-3]

The structural anisotropy inherent to high-index silicon surfaces makes them potentially significant substrates for electronic device fabrication.^{1–4} Of the planar surfaces between (001) and (111),^{5–8} Si(114) has the simplest structure and a surface energy comparable to Si(001).⁷ Given its natural anisotropic “single-domain” structure (see Fig. 1), Si(114) should make an interesting substrate for heteroepitaxy.

The potential of Si(114) as a substrate would be greatly enhanced if it could be easily hydrogen terminated. Hydrogen can be used to reduce surface contamination and interface states,^{9,10} and can also serve as a surfactant¹¹ and as an electron-beam lithography mask for nanoelectronic structures.^{12–15} However, to our knowledge Si(001) is the only Si surface that can be easily monohydride terminated with gaseous hydrogen.¹⁶ On high-index surfaces the H-surface chemistry is generally complex, a consequence of the heterogeneity of the potential binding sites.^{17,18} Even on the low-index Si(111) face the complexity of the (7×7) reconstruction is such that a monohydride surface can only be achieved using extreme exposure conditions, with a high-density of defects remaining on the resulting surface.^{16,19}

In this letter we describe the adsorption of H on Si(114) as characterized by scanning tunneling microscopy (STM) and first-principles calculations. Despite the relatively complex structure of Si(114), we find that a well-ordered, low-defect-density monohydride surface can be easily made, and that this surface can be uniformly patterned with low-voltage electrons.

The experiments were performed in ultrahigh vacuum using Si wafers oriented to within 0.3° of (114). The surfaces were cleaned by heating in vacuum to ~1225 °C for 60 s. Sample temperatures were determined based on the sample heating power, which was calibrated using both an infrared pyrometer and thermocouple measurements (the estimated uncertainties are ±25° below 500 °C and ±10° above). Atomic hydrogen exposure was performed by dissociating H₂ (typically, 2×10⁻⁵ Torr) with a hot W filament located ~1 cm from the surface. After the exposure, the samples were held at the deposition temperature in vacuum for at

least 5 min. Although STM images of both empty and filled electronic states have been acquired at room temperature, only filled-state images are shown here.

To determine the equilibrium surface geometry of the H-terminated Si(114) surface, we performed first-principles calculations within the local-density approximation (LDA) to density-functional theory. The calculations used a double-sided slab geometry consisting of ten Si layers plus hydrogen. All but the inner two layers were completely relaxed until the surface energy was converged to within 1 meV/Å². Total energies and forces were calculated using Troullier–Martins pseudopotentials in a plane-wave basis with a kinetic-energy cutoff of 12 Ry, as implemented in the FHI96MD code.²⁰ STM images were simulated by computing the surfaces of constant-energy-integrated local density of states.

In order to understand any changes induced by H adsorption on Si(114), it is useful to review the characteristics of the clean surface as observed with STM. As shown in Fig. 1, Si(114)-(2×1) terraces are composed of a periodic array of row-like structures oriented along the $[\bar{1}10]$ direction. Rows composed of three structures are observed: rebonded double-layer *B*-type (*D_B*) steps (*R*); tetramers (*T*), each made up of a dimer bonded to a nonrebonded *D_B* step; and isolated

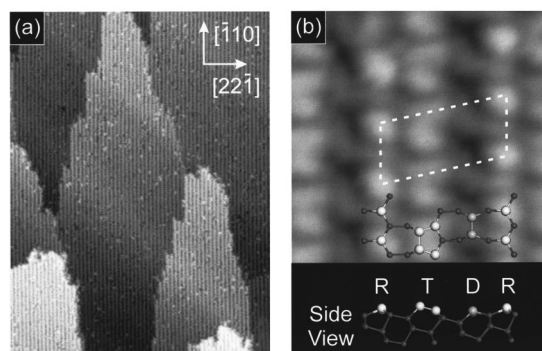


FIG. 1. Filled-state STM images of clean Si(114). (a) 106 nm×142 nm image showing periodically spaced rows *always* oriented along the $[\bar{1}10]$ direction. (b) 3.7 nm×3.7 nm image with structural model highlighting the three motifs that make up the (2×1) reconstruction: rebonded double-layer *B*-type (*D_B*) step (*R*); tetramer (*T*), made up of a dimer bonded to a nonrebonded *D_B* step; and isolated dimer (*D*). One primitive unit cell is outlined.

^{a)}Electronic mail: laracuen@stm2.nrl.navy.mil

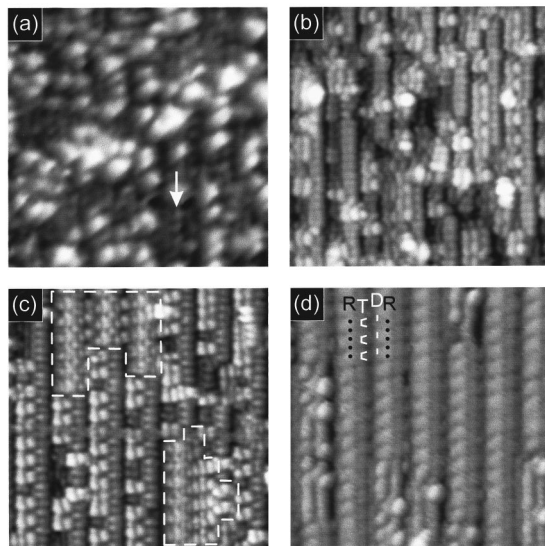


FIG. 2. 11.5 nm \times 11.5 nm filled-state STM images of Si(114) following H exposure (H_2 with a hot filament) at various substrate temperatures. (a) 10 L exposure at room temperature. The arrow indicates a row of unreacted Si atoms. (b) 480 L at 250 $^{\circ}$ C. (c) 480 L at 300 $^{\circ}$ C. Two different types of (2 \times 1) domains are outlined. (d) 240 L at 420 $^{\circ}$ C. A well-ordered H-terminated (2 \times 1) surface.

dimers (D). All three structures are buckled along $[\bar{1}10]$, with the “up” rebonded step atoms (every other one) corresponding to the brightest, spherical protrusions in the gray-scale STM images. Tetramers appear as an asymmetrical pair of lobes oriented perpendicular to the $[\bar{1}10]$. The isolated dimers are the darkest protrusions in the images, consistent with their relative structural height within the unit cell.

The changes induced by atomic hydrogen adsorption on Si(114)-(2 \times 1) are illustrated in Fig. 2, where images recorded following exposures at different temperatures are displayed. Room-temperature exposure disrupts the atomic-scale features [Fig. 2(a)], leaving about 60% of the surface covered with \sim 1-nm-high protrusions. Although unreacted regions can be seen between these features, they disappear after \sim 20 L total exposure. With further exposure at room temperature the protrusions get larger, increasing the surface roughness (not shown), similar to what is observed for H on Si(001).¹⁶ Increasing the surface temperature reduces the disorder caused by H adsorption, so that following exposure at 250 $^{\circ}$ C the large protrusions that appear at room temperature are mostly absent [Fig. 2(b)]. Under these conditions multiple layers of Si react with H, as indicated by the presence of dimer-like features oriented in *both* the $[\bar{1}10]$ and $[2\bar{2}\bar{1}]$ directions and the range of heights within the images. Exposure at 300 $^{\circ}$ C produces a surface with noticeably better atomic-scale order [Fig. 2(c)], with two distinct (2 \times 1)-like morphologies [outlined in Fig. 2(c)]. Similar to surfaces exposed at 250 $^{\circ}$ C, dimer-like features are observed oriented in both directions. Although the specific H-termination state of these structures is not known, the relative heights and lateral spacing of the two orientations of dimer-like features observed indicate that they arise from a splitting of double-layer D_B steps (R and T) into two adjacent single-layer steps ($S_A + S_B$).

In contrast to the effects of H at lower temperatures, exposure above 400 $^{\circ}$ C produces a well-ordered, low-defect-

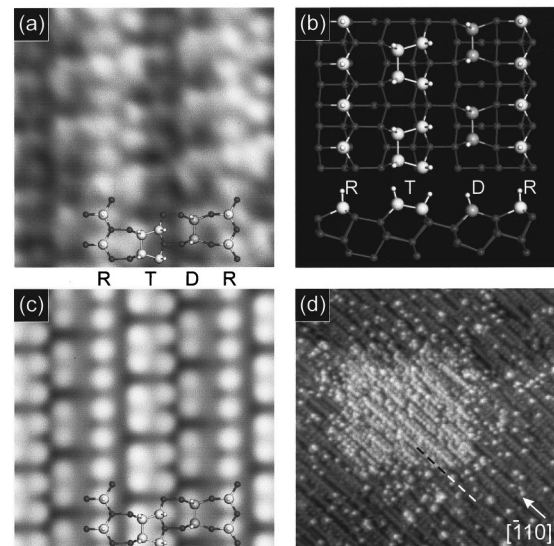


FIG. 3. (a) Atomic-resolution filled-state STM image of Si(114):H-(2 \times 1) produced at 420 $^{\circ}$ C (2 V, 3.7 nm \times 3.7 nm). The proposed structural model is overlaid and shown in detail in (b) using the theoretically relaxed geometry. (c) Simulated filled-state image (2 V) calculated for this structure. (d) 38 nm \times 38 nm image showing an area 19 nm \times 19 nm where H has been removed by scanning with a sample bias of 7 V. The dashed line is a guide to the eye along one rebonded double-layer step.

density, single-domain (2 \times 1)-reconstructed Si(114) surface, as shown in Fig. 2(d). The overall morphology of this surface, i.e., terrace size, defect density, and periodic corrugation, is so similar to that of the clean surface that images on the \sim 100 nm scale are indistinguishable from Fig. 1(a). At higher magnifications, however, differences on the atomic scale become apparent [compare Fig. 1(b) with Fig. 3(a)], especially in the highest rows. Whereas on the clean surface the 2 \times row of alternately buckled rebonded atoms stands out, on the H-terminated surface a row with a nearly 1 \times periodicity is observed between rows of dimer-like structures, all with similar heights in the filled-state images.

On Si(001)-(2 \times 1) gaseous atomic H reacts with the dangling bonds to produce $Si_{4-n}H_n$ ($n=1, 2, 3$) species, with the relative composition dependent on adsorption temperature.^{21–24} Room-temperature adsorption etches the surface, producing a rough, disordered mixture of hydrides.¹⁶ Under certain H-exposure conditions, a well-ordered (3 \times 1) surface can be prepared at \sim 130 $^{\circ}$ C, with alternating dihydride- and monohydride-terminated dimers.^{16,25,26} The surface coverage of the monohydride phase increases with exposure temperature, culminating about 400 $^{\circ}$ C in a nearly perfect monohydride-passivated Si(001):H-(2 \times 1) surface composed of H–Si–Si–H dimer rows. In general, the reaction of atomic H with Si(114) appears qualitatively similar to Si(001)—producing rough disorder at low temperatures and more homogeneous, ordered structures with increasing temperature—suggesting that similar atomic-scale reactions occur. It appears that room-temperature exposure etches the (114) surface (we assume that the various indistinct clusters observed on the surface are silicon hydrides). At higher temperatures, H adsorption produces more well-ordered structures. Although the atomic-scale structures of the different features observed following exposure between 200 and 350 $^{\circ}$ C are not known, we suspect that they are associated

with locally ordered combinations of mono- and dihydride dimers and step structures. In contrast to Si(001), a dihydride reconstruction with long-range order is not observed on this surface. Additional surface characterization including vibrational spectroscopy is planned to more definitively identify these H–Si structures.

When we expose Si(001) to H under conditions identical to those used to produce the well-ordered Si(114):H-(2×1) structure [Figs. 2(d) and 3(a)], a nearly perfect Si(001):H-(2×1) monohydride surface results (not shown). Combining our STM results with LDA calculations, we have determined that the Si(114):H-(2×1) produced under these conditions is also a simple monohydride-terminated surface. The structure of this (2×1) surface is essentially that of the clean surface with each dangling bond (db) capped by a single H atom [Fig. 3(b)]. The first-principles calculations show that this structure readily relaxes into a low surface energy configuration, and the corresponding simulated STM images accurately reproduce the general appearance of the atomic-scale features [Fig. 3(c)]. The main effect of the H on Si(114) is to remove the buckling, which on the clean surface is driven by charge transfer between the otherwise half-filled dbs. With H saturating each db, there is no charge-related driving force for buckling; as a consequence, the rebonded atoms (*R*) and the adjacent dimers (*D* and dimer half of *T*) relax to similar heights. This relaxation changes the relative prominence of the different features in the STM images, with the rebonded and dimer rows become relatively equal in height. The nonrebonded step within the H-terminated tetramers usually appears as the lowest feature (although the heights are somewhat variable with tunneling conditions).

Given the relative complexity of the (114) surface structure, it is surprising that the surface can be so easily and uniformly terminated with H. On the clean Si(114)-(2×1) surface the rebonding atoms serve to halve the density of the dbs at the underlying double-layer steps, albeit at the expense of additional surface stress. Because H can saturate every db without requiring strained Si bonds, one might expect H exposure to remove the rebonding atoms (leaving a H-terminated step). In fact, although the rebonding atoms remain on Si(114) following high-temperature exposure to H, we have found that on surfaces oriented closer to (001)—where the double steps are separated by three or more dimers—most of the rebonding atoms are stripped off. The “unrebonding” of the double-layer steps on these surfaces has a destabilizing effect, dramatically altering the step energetics and thereby the overall surface morphology. (This phenomenon will be discussed in more detail in a separate publication.)

The ability to simply H terminate each db on the clean Si(114)-(2×1) surface implies that the three different structures, (001)-like dimers, rebonded double-layer steps, and

nonrebonded double-layer steps, each react similarly with H under appropriate conditions. A significant consequence of this unexpected homogeneity is the ability to selectively pattern the surface by using the STM probe to *uniformly* desorb H. Removal of the H in this way exposes a relatively well-ordered area with the usual clean surface structure, as shown in Fig. 3(d). As expected, the H-free regions appear higher in the filled-state image, with the buckled rebonded rows restored to prominence. Although we have not investigated such lithography on Si(114):H as exhaustively as has been done for Si(001):H, we expect a similar degree of control will be possible. These results set the stage for further investigations of Si(114) as a substrate for electronic applications.

Computational work was supported by grants of HPC time from the DoD Shared Resource Centers MAUI and WPASC. This work was funded by ONR and a NRL/NRC postdoctoral fellowship (A.L.).

- ¹S. Rujirawat, L. A. Almeida, Y. P. Chen, and S. Sivananthan, Appl. Phys. Lett. **71**, 1810 (1997).
- ²P. Waltereit, J. M. Fernández, S. Kaya, and T. J. Thornton, Appl. Phys. Lett. **72**, 2262 (1998).
- ³M. J. Jurkovic, J. Alperin, Q. Du, W. I. Wang, and M. F. Chang, J. Vac. Sci. Technol. B **16**, 1401 (1998).
- ⁴R. M. Sieg, S. A. Ringel, S. M. Ting, S. B. Samavedam, M. Currie, T. Langdo, and E. A. Fitzgerald, J. Vac. Sci. Technol. B **16**, 1471 (1998).
- ⁵J. Dabrowski, H.-J. Mussig, and G. Wolff, Surf. Sci. **331-333**, 1022 (1995).
- ⁶A. A. Baski, S. C. Erwin, and L. J. Whitman, Science **269**, 1556 (1995).
- ⁷S. C. Erwin, A. A. Baski, and L. J. Whitman, Phys. Rev. Lett. **77**, 687 (1996).
- ⁸A. A. Baski, S. C. Erwin, and L. J. Whitman, Surf. Sci. **392**, 69 (1997).
- ⁹T. Hsu, B. Anthony, R. Qian, J. Irby, S. Banerjee, A. Tasch, S. Lin, H. Marcus, and C. Magee, J. Electron. Mater. **20**, 279 (1991).
- ¹⁰J. W. Lyding, K. Hess, and I. C. Kizilyalli, Appl. Phys. Lett. **68**, 2526 (1996).
- ¹¹S.-J. Kahng, Y. H. Ha, J.-Y. Park, S. Kim, D. W. Moon, and Y. Kuk, Phys. Rev. Lett. **80**, 4931 (1998).
- ¹²J. W. Lyding, T.-C. Shen, J. S. Hubacek, J. R. Tucker, and G. C. Abeln, Appl. Phys. Lett. **64**, 2010 (1994).
- ¹³T.-C. Shen, C. Wang, G. C. Abeln, J. R. Tucker, J. W. Lyding, P. Avouris, and R. E. Walkup, Science **268**, 1590 (1995).
- ¹⁴D. P. Adams, T. M. Mayer, and B. S. Swartzentruber, J. Vac. Sci. Technol. B **14**, 1642 (1996).
- ¹⁵T.-C. Shen, C. Wang, and J. R. Tucker, Phys. Rev. Lett. **78**, 1271 (1997).
- ¹⁶J. J. Boland, Adv. Phys. **42**, 129 (1993).
- ¹⁷J. H. Wilson, P. D. Scott, J. B. Pethica, and J. Knall, J. Phys.: Condens. Matter **3**, S133 (1991).
- ¹⁸A. A. Baski and L. J. Whitman, J. Vac. Sci. Technol. A **13**, 1469 (1995).
- ¹⁹F. Owman and P. Martensson, Surf. Sci. **303**, L367 (1994).
- ²⁰M. Bockstedte, A. Kley, and M. Scheffler, Comput. Phys. Commun. **107**, 187 (1997).
- ²¹S. Maruno, H. Iwasaki, K. Horioka, L. Sung-te, and S. Nakamura, Phys. Rev. B **27**, 4110 (1983).
- ²²Y. J. Chabal and K. Raghavachari, Phys. Rev. Lett. **54**, 1055 (1985).
- ²³S. M. Gates, R. R. Kunz, and C. M. Greenlief, Surf. Sci. **207**, 364 (1989).
- ²⁴C. C. Cheng and J. T. Yates, Jr., Phys. Rev. B **43**, 4041 (1991).
- ²⁵J. E. Northrup, Phys. Rev. B **44**, 1419 (1991).
- ²⁶D. T. Jiang, G. W. Anderson, K. Griffiths, T. K. Sham, and P. R. Norton, Phys. Rev. B **48**, 4952 (1993).